All-*trans* retinoic acid alters the expression of the tight junction proteins Claudin-1 and -4 and epidermal barrier function-associated genes in the epidermis

JING LI, QIANYING LI and SONGMEI GENG

Department of Dermatology, Northwest Hospital, Xi'an Jiaotong University, Xi'an, Shaanxi 710004, P.R. China

Received September 12, 2018; Accepted February 12, 2019

DOI: 10.3892/ijmm.2019.4098

Abstract. All-*trans* retinoic acid (ATRA) regulates skin cell proliferation and differentiation. ATRA is widely used in the treatment of skin diseases, but results in irritation, dryness and peeling, possibly due to an impaired skin barrier, although the exact mechanisms are unclear. The present study established an ATRA-associated dermatitis mouse model (n=32) in order to examine the molecular mechanisms of skin barrier impairment by ATRA. Changes in epidermal morphology and structure were observed using histological examination and transmission electron microscopy (TEM). Gene expression was analyzed by microarray chip assay. Histology and TEM demonstrated pronounced epidermal hyperproliferation and parakeratosis upon ATRA application. The stratum corneum layer displayed abnormal lipid droplets and cell-cell junctions, suggesting alterations in lipid metabolism and dysfunctional cell junctions. Gene expression profiling revealed that factors associated with epidermal barrier function were differentially expressed by ATRA, including those associated with tight junctions (TJs), cornified envelopes, lipids, proteases, protease inhibitors and transcription factors. In the mouse epidermis, Claudin-1 and -4 are proteins involved in TJs and have key roles in epidermal barrier function. ATRA reduced the expression and altered the localization of Claudin-1 in HaCaT immortalized keratinocytes and the mouse epidermis, which likely leads to the disruption of the epidermal barrier. By contrast, Claudin-4 was upregulated in HaCaT cells and the mouse epidermis following treatment with ATRA. In conclusion, ATRA exerts a dual effect on epidermal barrier genes: It downregulates the expression of Claudin-1 and upregulates the expression of Claudin-4. Claudin-4 upregulation may be a compensatory response for the disrupted barrier function caused by Claudin-1 downregulation.

Correspondence to: Dr Songmei Geng, Department of Dermatology, Northwest Hospital, Xi'an Jiaotong University, 157 Xi Wu Road, Xi'an, Shaanxi 710004, P.R. China
E-mail: gsm312@yahoo.com

Abbreviations: ATRA, all-*trans* retinoic acid; TEM, transmission electron microscopy; TJs, tight junctions; GO, Gene Ontology; DMSO, dimethyl sulfoxide; EDC, epidermal differentiation complex; SPRRs, small proline-rich region proteins; FLG, filaggrin; LOR, loricrin

Key words: ATRA, skin irritation, TJ, barrier function, Claudin-1, Claudin-4

Introduction

All-*trans* retinoic acid (ATRA) exerts essential roles in reproduction, embryogenesis, cell proliferation, differentiation and apoptosis (1,2). ATRA also regulates skin function and is widely used for the treatment of skin diseases such as acne, psoriasis, ichthyosis and skin cancer (3-5), but its clinical application is limited by adverse skin reactions, including erythema, scaling, dryness, desquamation and vessel dilation. These reactions are potentially associated with epidermal barrier dysfunction (6), but the mechanisms are largely unknown.

Tight junctions (TJs) in epithelial and endothelial tissues have been well studied, and a previous study suggested that the TJs of the stratum granulosum (SG) are responsible for the protective function of epithelial tissues (7). TJs consist of transmembrane Claudins, adherent junction (AJ) molecules, occludin, plaque proteins (e.g. zonula occludens-1, -2 and -3, and multiple PDZ domain protein), and cell polarity complex proteins [e.g. the protein kinase C ι-type/partitioning defective 3 homolog (Par3)/Par6 complex] (8). Claudins contain two extracellular loops (cytoplasmic C- and N-terminal) and four transmembrane domains (9,10). Claudins-1, -2, -4 and -6 are essential for TJ formation and are involved in the barrier to paracellular transport (9,11-14). The roles of Claudins in barrier function have been addressed in epithelial cell cultures and Claudin-knockout/transgenic mice (15,16). Claudin-1 and -4 are concentrated in TJs (17). Continuous Claudin-based TJs are present in the epidermis and these particular TJs are crucial for the barrier function of mammalian skin (17). In addition, Claudin-1 and -4 are involved in the pathogenesis of skin lesions (18-20). How Claudin-1 and -4 are regulated in response to ATRA is largely unknown.

To understand the molecular basis of ATRA-induced barrier dysfunction, a gene expression array was used to observe the differential gene expression in mouse skin and HaCaT cells following treatment with ATRA. Using a mouse model and a

gene expression array, it was demonstrated that ATRA does, in fact, alter the structure of TJs in mouse skin. Therefore, the hypothesis was that Claudins possibly exert an essential role in barrier dysfunction during ATRA-induced skin irritation. The present study aimed to investigate the molecular mechanisms of barrier dysfunction during ATRA-induced skin irritation.

Materials and methods

Animals. Male BALB/c mice (n=32; 8 weeks of age; weight, ~25 g) were obtained from Xi'an Jiaotong University Animal Center (Xi'an, China). The mice were fed standard chow and had access to water *ad libitum*, and were caged in a controlled environment (12 h light/dark cycle; temperature, 20-25˚C; humidity, 45-55%). The mice were acclimatized for 3 days prior to any experiments. All experimental procedures were performed in accordance with the 'Principles of Laboratory Animal Care' (NIH) and with the approval of the laboratory animal care committee of Xi'an Jiaotong University (no. XJTULAC2017-733).

Animal treatment. The skin on the backs of the mice was shaved using an electric shaver. The mice were divided into two group: i) Treated with topical 0.1% ATRA cream (Chongqing Winbond Pharmaceutical Co., Ltd., Chongqing, China) twice a day; and ii) treated with an oil/water cream (vehicle control) twice a day. The Psoriasis Area and Severity Index (PASI) scoring system was used to assess the severity of inflammation on the back skin of the mice (21). The PASI is widely used in clinical practice. Erythema, scales and thickening are scored as follows: 0, absent; 1, slight; 2, mild; 3, obvious; and 4, very obvious. The sum of the scores of these three factors is an indicator of the severity of inflammation (score of 0-12).

After 5 days of treatment, the mice were anesthetized using pentobarbital at 50 mg/kg. The skin from the backs of the mice, including the dermis and subcutaneous tissues, was removed. The skin was washed with pre-cooled PBS, excess fat was removed, and the specimens were placed in liquid nitrogen for RNA extraction. Subsequently, the mice were sacrificed by cervical dislocation.

Histological and ultrastructural analysis. ATRA-treated and untreated mouse dorsal skin specimens (1x1.5 cm) were fixed in 4% paraformaldehyde for 24 h at 4˚C, dehydrated and embedded in paraffin. The samples were sectioned at 7 μm and stained with hematoxylin for 5 min and eosin for 2 min at room temperature. The epidermal thickness, parakeratosis, spongiosis and degree of inflammation were evaluated. Spongiosis (presence of widened intracellular spaces between epidermal keratinocytes) and inflammation were evaluated on a scale of 0-4. Epidermal thickness and spongy edema were measured using the built-in measurement tool in the software ndp.view2 (Hamamatsu Photonics K.K., Hamamatsu, Japan; https://www.hamamatsu.com/jp/en/product/type/U12388-01.html; version 2.7). The expanded capillaries were counted at high magnification (x200) in 10 randomly selected fields under an Olympus BX51 light microscope equipped with a DP70 digital camera (Olympus Corporation, Tokyo, Japan). Incomplete keratinization was assessed as present or absent (22).

The specimens were cut into 1-cm blocks and dipped in ice-cold sodium cacodylate buffer solution containing 2.5% glutaraldehyde at 4˚C for 24 h. The blocks were washed three times and treated with 1% osmium tetroxide at 4˚C for 1 h. The samples were dehydrated using an ethanol series and embedded in Epon 812. Ultra-thin sections were stained with lead citrate for 10 min and uranyl acetate for 30 min at room temperature. Ultrastructural changes were observed by transmission electron microscopy (TEM) using a H7650 microscope (Hitachi, Ltd., Tokyo, Japan).

Cell culture and treatment. HaCaT cells (immortalized keratinocytes) were obtained from the Fourth Military Medical University (Shan'xi, China) and grown in RPMI-1640 (GE Healthcare, Chicago, IL, USA) with 10% fetal bovine serum (Life Technologies; Thermo Fisher Scientific, Inc., Waltham, MA, USA) and 1% penicillin-streptomycin (GE Healthcare). Short tandem repeat profiling was performed by Shanghai Zhong Qiao Xin Zhou Biotechnology Co., Ltd. (Shanghai, China) to validate the cell line. The cells were subcultured following dissociation with 0.25% trypsin/0.05% EDTA (1:1) and passaged at a ratio of 1:4 every 3 days.

HaCaT cells (5,000 cells/well) were incubated in 96-well plates for 48 h and treated by different concentrations (0.1, 0.5, 1, 5 and 10 μM) of ATRA at 37˚C for a further 36 h. A volume of 20 μl MTT solution (5 mg/ml) was added to each well and the culture continued for 4 h. Subsequently, the medium was removed, and 150ul dimethyl sulfoxide (DMSO) was added to each well. The light absorption value of each well was measured at optical density 490 nm (570 nm) with a micro-plate reader. Following determination of the half-maximal inhibitory concentration using different concentrations of ATRA (Sigma-Aldrich; Merck KGaA, Darmstadt, Germany), HaCaT cells were incubated with or without 1 μM ATRA for 36 h at 37˚C, which was chosen for use in the subsequent experiments. Stock solutions of ATRA (0.01 M) were prepared in DMSO, stored in the dark at -20˚C, and further diluted with RPMI-1640. The concentration of DMSO was 1‰.

Microarray analysis. Microarray analysis was used primarily to identify candidates that were later confirmed via reverse transcription-quantitative polymerase chain reaction (RT-qPCR) and/or immunohistochemistry. The gene expression profiles in the skin of mice and in HaCaT cells treated or untreated with ATRA were compared using NimbleGen Gene Expression analysis (Nimblegen Systems Inc., Madison, WI, USA). The ds-cDNA samples were washed and labeled according to the Nimblegen Gene Expression Analysis protocol (Nimblegen Systems Inc.). A NanoDrop ND-1000 was used to quantify the cDNA following purification. Cy3 labeling was conducted using the NimbleGen One-Color DNA labeling kit (NimbleGen Systems, Inc.), according to the manufacturer's protocol. Subsequently, 100 U Klenow fragment (New England Biolabs, Inc., Ipswich, MA, USA) and 100 pmol deoxynucleoside triphosphates were added and incubated at 37˚C for 2 h. One-tenth volume of 0.5 M EDTA was added to stop the reaction. The labeled ds-cDNA was purified using isopropanol/ethanol precipitation. The microarrays were immersed in the NimbleGen hybridization buffer/hybridization component A, which was supplemented with 4 μg

ds-cDNA with Cy3 labeling. The reaction system was kept in a hybridization chamber (Nimblegen Systems, Inc.) at 42˚C for 4 h. The NimbleGen Wash Buffer kit (Nimblegen Systems, Inc.) was used to wash the microarrays in an environment without ozone. The Axon GenePix 4000B microarray scanner was used to scan the microarrays.

RT-qPCR. The RNAeasy Midi kit (Qiagen AB, Sollentuna, Sweden) was used to isolate the total mRNA, according to the manufacturer's protocol. RNA (1 μg) was added in a 20-μl reaction system (PrimeScript RT Reagent Kit; Takara, Otsu, Japan) at 37˚C for 15 min and 85˚C for 5 sec for cDNA synthesis. The SYBR Premix Ex Taq II amplification kit (Perfect Real Time; Takara Biotechnology Co., Ltd., Dalian, China) was used for qPCR on a Bio-Rad IQ5 System (Bio-Rad Laboratories, Inc., Hercules, CA, USA). The conditions were: i) 95˚C denaturation for 10 min; and ii) 40 cycles at 95˚C for 10 sec and 60˚C for 30 sec. The primers are listed in Table I. β-actin was used for normalization. The results were analyzed using the IQ5 software (version 2.5). Gene expression levels were calculated using the $2^{-\Delta\Delta Cq}$ method (23).

Table I. Primers for reverse transcription-quantitative polymerase chain reaction.

Gene symbol	Primers
β-actin	F-5'-AGCAGAGAATGGAAGAGTAAA-3'
	R-5'-ATGCTGCTTACATGTCTCGAT-3'
CLDN4	F-5'-TATGGATGAACTGCGTGGTG-3'
	R-5'-GATGATGVTGATGATGACGAG-3'
CLDN1	F-5'-GAAGTGTATGAAGTGCTTGG-3'
	R-5'-GGGTCATAGGGTCATAGAAT-3'
CLDN2	F-5'-GTGAAGGCAGAGATGAGAAGAGG-3'
	R-5'-ATGGGATTTGGGCTTTTGG-3'
FLG	F-5'-AGACTGGGAGGCAAGCTACAAC-3'
	R-5'-TGGTTTGGAGTGGGATTGCT-3'

F, forward; R, reverse; CLDN, Claudin; FLG, filaggrin.

Western blotting. ATRA-treated and untreated HaCaT cells were lysed in radioimmunoprecipitation assay buffer [150 mM NaCl, 50 mM Tris-HCl (pH 8.0), 0.5% deoxycholate, 0.1% SDS, 1% Nonidet P-40 and protease inhibitor cocktail; Sigma-Aldrich; Merck KGaA] at 4˚C for 1 h. Protein concentration was measured using a bicinchoninic acid protein assay kit (Beyotime Institute of Biotechnology, Haimen, China). Equal amounts of proteins (30 μg) were separated on 12% SDS-PAGE gels and transferred to PVDF membranes (EMD Millipore, Billerica, MA, USA). TBS buffer containing Tween-20 (TBST) and 5% non-fat milk was used to block non-specific binding at room temperature for 2 h. Following blocking, primary antibodies were incubated overnight at 4˚C: Rabbit anti-human Claudin-1 (cat. no. 13050-1-AP; ProteinTech Group, Inc., Chicago, IL, USA; 1:200), goat anti-human Claudin-4 (cat. no. 17664; Santa Cruz Biotechnology, Inc., Dallas, TX, USA; 1:200) and mouse anti-human β-actin (cat. no. 47778; Santa Cruz Biotechnology, Inc.; 1:1,000). The membranes were washed three times with TBST for 5 min. Horseradish peroxidase (HRP)-conjugated Affinipure Rabbit Anti-Goat IgG (H+L) (cat. no. SA00001-2; ProteinTech Group, Inc.; 1:3,000), HRP-conjugated Affinipure Goat Anti-Mouse IgG (H+L) (cat. no. SA00001-1; ProteinTech Group, Inc.; 1:3,000) and HRP-conjugated Affinipure Donkey Anti-Goat IgG (H+L) (cat. no. SA00001-3; ProteinTech Group, Inc.; 1:4,000) were incubated for 1 h at 37˚C prior to visualization with enhanced chemiluminescence (Amersham; GE Healthcare). Densitometry was used to quantify the signal intensities using Quantity One 4.5 software (Bio-Rad Laboratories, Inc.). All measurements were performed in triplicates from three independent experiments.

Immunofluorescence. HaCaT cells and cryostat sections (4 μm) of skin from ATRA-treated and untreated mice were fixed in ice-cold 4% paraformaldehyde in PBS for 30 min. Non-specific binding was blocked with 10% normal goat serum (OriGene Technologies, Inc., Beijing, China) for 20 min at 37˚C. Goat anti-human Claudin-4 (1:50) and rabbit anti-human Claudin-1 antibodies (1:50) were incubated overnight at 4˚C. PBS was used as a negative control. The sections were washed twice for 5 min in PBS. Alexa Fluor 594-labeled secondary antibodies (cat. nos. A32758 and A32740; Jackson ImmunoResearch Laboratories, Inc., West Grove, PA, USA; 1:200) were incubated for 1 h at room temperature and revealed using DAPI (1:5,000 in PBS) for 2 min at room temperature. A laser scanning confocal microscope (LSM510; Zeiss AG, Oberkochen, Germany) was used to capture images of the cells (x200 magnification).

Statistical analysis. All statistical analyses were conducted using SPSS 16.0 (SPSS, Inc., Chicago, IL, USA). Data are expressed as the mean ± standard deviation. All measurements were performed in triplicate from three independent experiments. The distribution was tested for normality using the Kolmogorov-Smirnov test. Statistical significance was evaluated by independent sample t-test for normally distributed data and using the Mann-Whitney U test for non-normally distributed data. $P<0.05$ was considered to indicate a statistically significant difference.

For the microarray data, the NimbleScan software (version 2.5; NimbleGen Systems, Inc.) was used to conduct grid alignment and analyze the expression profiles. The Robust Multichip Average (RMA) algorithm and quantile normalization in NimbleScan software were applied to the normalized expression data. The gene levels were inputted into the Agilent GeneSpring software (version 12.0; Agilent Technologies, Inc., Santa Clara, CA, USA). Fold-change filtering was applied for the identification of genes with differential expression levels. The threshold was set at-fold-change ≥2.0. The Agilent GeneSpring GX software (version 12.0; Agilent Technologies, Inc.) was used to conduct hierarchical clustering. The roles of the differentially expressed genes were determined using Gene Ontology (GO; www.geneontology.org) and pathway analyses (https://www.genome.jp/kegg) conducted on the basis of the standard enrichment computation method, and using Fisher's exact test to determine whether the amount of overlaps between the GO annotation list and the list of differentially

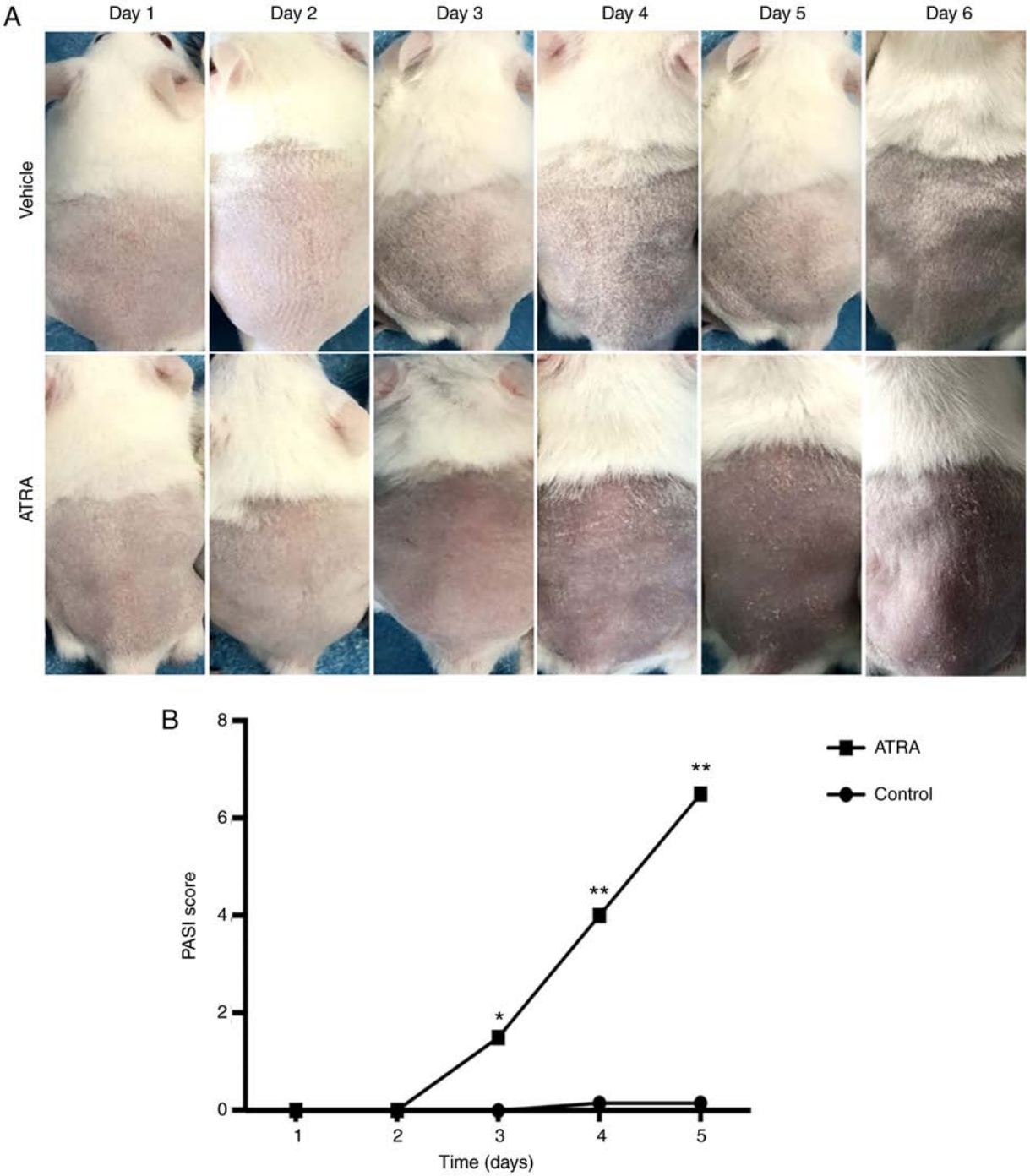

Figure 1. Effect of ATRA on morphological changes and PASI score on the back skin of mice. (A) After 5 days of treatment, no obvious alterations were detected in the control skin. Circumscribed erythema occurred after 3 days of ATRA application and gradually expanded, presenting as fine flat scales covering the surface of the erythema and peaking at 5 days. (B) The PASI scoring system was used to assess the severity of inflammation on the back skin of the mice. *P<0.05, **P<0.01 vs. respective control. PASI, Psoriasis Area and Severity Index; ATRA, all-*trans* retinoic acid.

expressed genes was significant. P≤0.05 indicated that the GO term enrichment was statistically significant.

Results

Topical ATRA induces histological alterations in the skin of treated mice. After 5 days of treatment, no marked alterations were detected in the control skin. Circumscribed erythema occurred after 3 days of ATRA application (n=6), with fine flat scales covering the surface of the erythema that peaked at 5 days (Fig. 1). Hematoxylin and eosin staining of ATRA-treated skin demonstrated crust, focal parakeratosis, hyperproliferation and intercellular edema of the stratum spinosum (Fig. 2A). In the ATRA-treated dermis, large amounts of inflammatory cell infiltration and capillary dilation were observed (Fig. 2A). Epidermal thickness was 2.5 times higher following ATRA intervention compared with that of the control group (P<0.0001), in addition to increases in parakeratosis (P<0.001) and spongiosis (P<0.002). In the dermis, perivascular lymphocytic infiltration (P<0.002) and

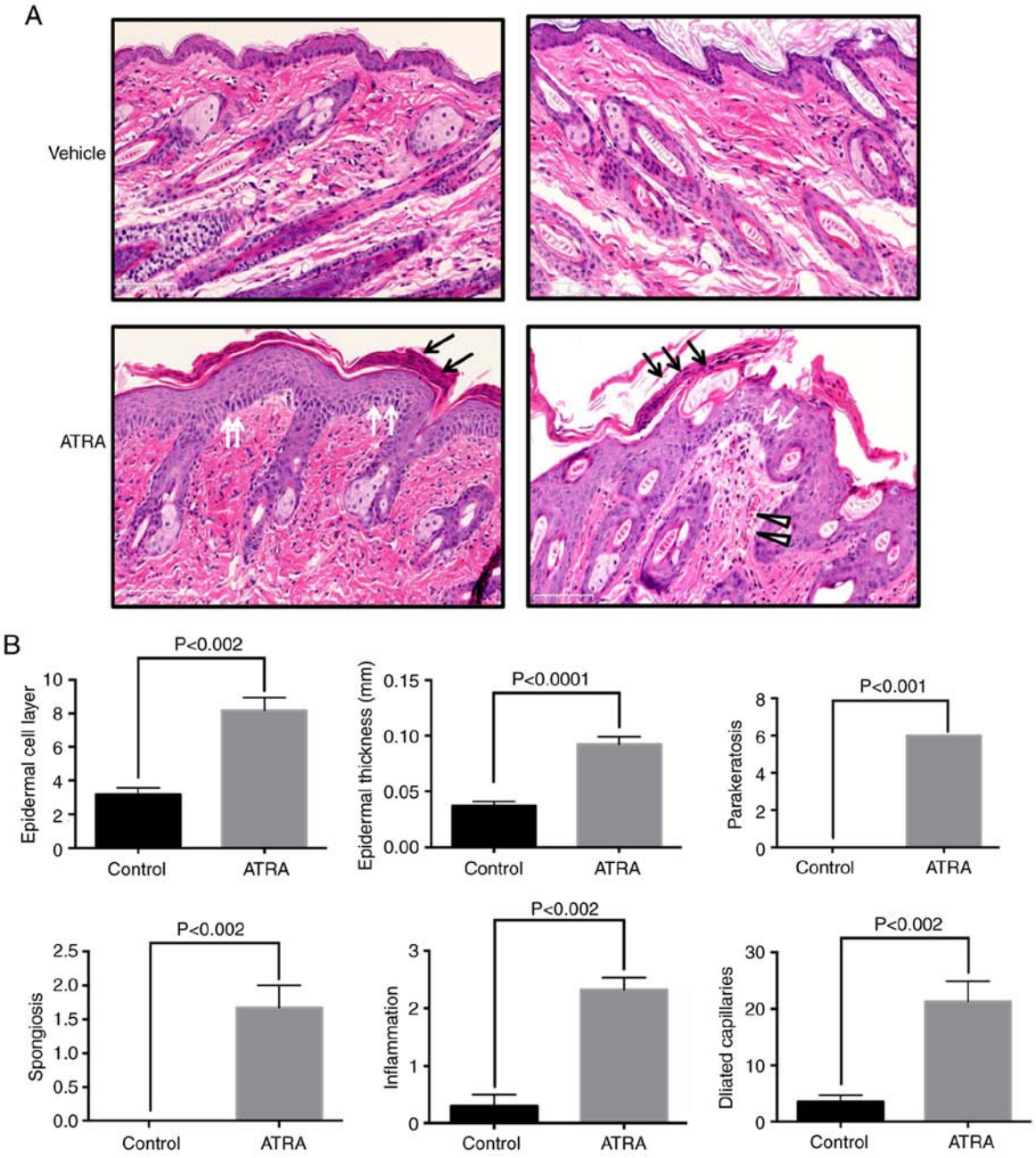

Figure 2. Effect of ATRA on histological changes in the mouse epidermis and quantitative analysis. (A) The mice were treated with topical 0.1% ATRA cream or oil/water cream (vehicle) twice a day. The mice were sacrificed after 5 days of ATRA treatment. The stratum corneum was impaired and the number of epidermal cell layers and epidermal thickness were increased in ATRA-treated mice. Parakeratosis (black arrows), intercellular edema (triangles), and dermal inflammatory cell infiltration (white arrows) were also observed. n=6 per group. Scale bar, 100 μm. A representative image was selected from each group. (B) Quantitative analysis of epidermal cell layers, epidermal thickness, parakeratosis spongiosis, perivascular lymphocytic infiltration and telangiectasia. ATRA, all-*trans* retinoic acid.

telangiectasia (P<0.002) were observed in the dermal papilla and in the superficial layer (Fig. 2B).

ATRA treatment causes ultrastructural abnormalities in the epidermis. Compared with control skin, keratohyalin granules were decreased in number in the SG (n=3; Fig. 3A). TEM also demonstrated that the keratinocyte cytoskeleton was damaged by ATRA and that the cytoskeletal network disappeared in the local upper stratum corneum (Fig. 3A). In the upper stratum corneum, multiple lipid droplets were observed in the cytoplasm of corneocytes in the ATRA-treated skin (Fig. 3B). In the epidermis of ATRA-treated skin, TEM revealed a disordered arrangement of stratum spinosum cells, in addition to the appearance of significantly larger nucleoli and wider intercellular spaces (Fig. 3B). Desmosomes were decreased and disordered in ATRA-treated skin (Fig. 3C). Quantitative analysis of keratohyalin granules, lipid droplets and desmosomes is presented in Fig. 3D.

Gene expression profiling reveals dysregulation of epidermal barrier-associated genes in the mouse epidermis and HaCaT cells treated with ATRA. With the aim of improving the

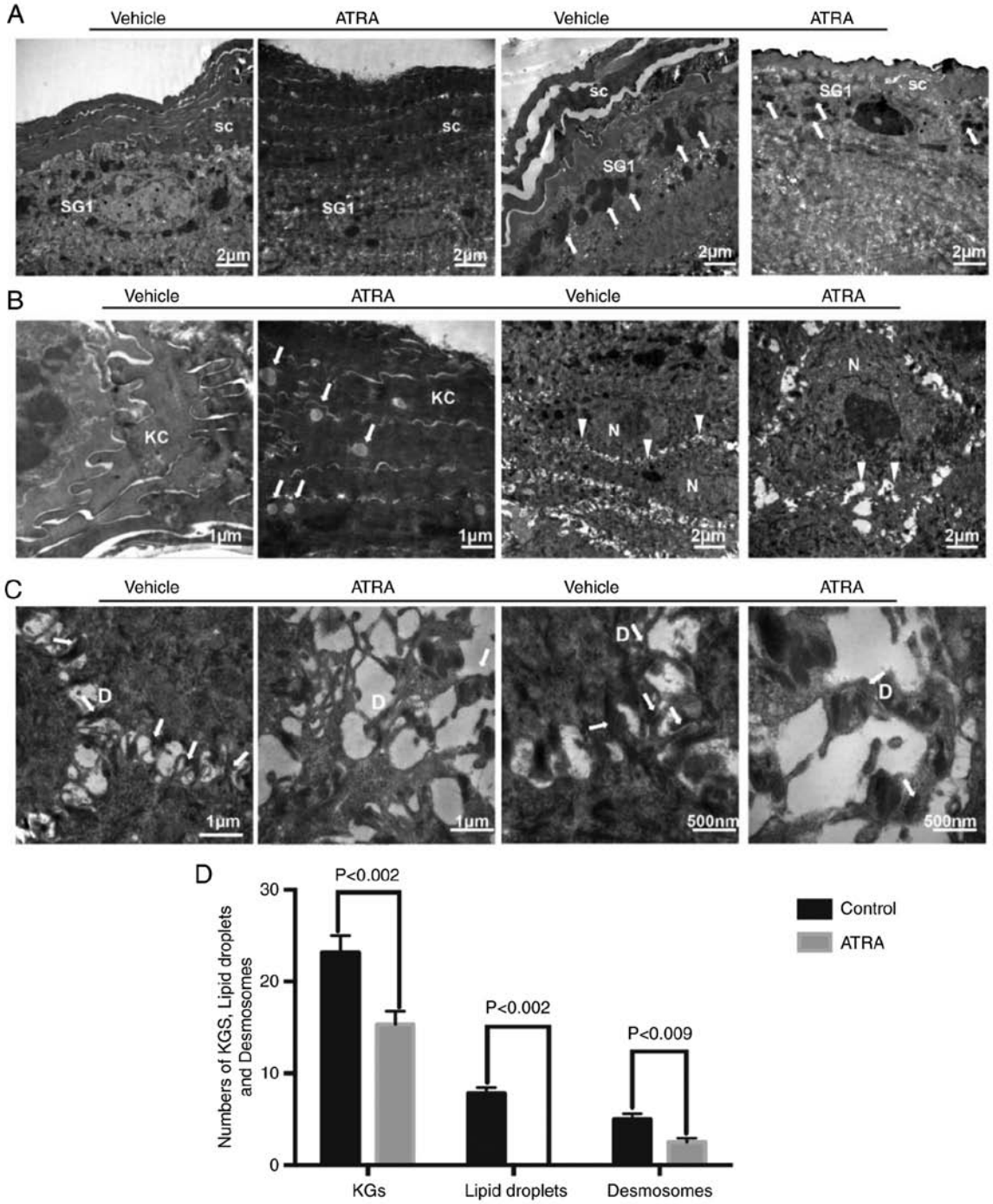

Figure 3. Effect of ATRA on ultrastructural alterations in the mouse epidermis. (A) The stratum corneum was impaired and the number of epidermal cell layers and epidermal thickness were increased. The number of KGs around granular cells were decreased (arrows). (B) There were multiple lipid droplets in the corneocytes (arrows). The volume of the spinous layer cells was increased, the nucleoli were significantly larger, and the intercellular space was widened (triangles). (C) Desmosomes were reduced in number and damaged (arrows). n=3/group. A representative image is presented for each group. (D) The numbers of KGs, lipid droplets and desmosomes were quantified. KC, keratinocyte; SC, stratum corneum; SG, stratum granulosum; D, desmosome; N, nucleus; KGs, keratinocyte granules; ATRA, all-*trans* retinoic acid.

understanding of the molecular mechanisms of ATRA-induced barrier dysfunction, gene expression array analysis (n=1) was used to identify candidate genes for barrier function in the mouse skin and HaCaT cells. There were 897 upregulated and 1,087 downregulated genes following treatment with ATRA in the mouse epidermis. Similarly, there were 1,220 upregulated and 905 downregulated genes following treatment with ATRA in HaCaT cells. The genes involved in epidermal barrier function were revealed by gene expression analyses and are presented in Tables II-V. The downregulated epidermal barrier-associated genes following treatment with ATRA in the mouse skin included genes involved in 'cornified envelope components', 'intermediate filament', 'lipid metabolic process', 'gap junction', 'tight junction' and 'desmosome' (Table II). The upregulated epidermal barrier-associated genes following treatment with ATRA in mouse skin included genes involved

Table II. Downregulation of epidermal barrier-associated genes following treatment with all-*trans* retinoic acid in mouse skin (n=1 per group;-fold change >2; P<0.05).

A, Cornified envelope components

GenBank accession no.	Gene name	Gene full name	Fold downregulation
AF510860	FLG	Filagrin	2.13
BC108980	FOXN1	Forkhead box N1	2.42
BC107019	SPRR4	Small proline-rich protein 4	2.67
BC109181	LCE1M	Late cornified envelope 1M	6.64
BC031486	PPHLN1	Periphilin 1	2.40
BC119192	GPRC5D	Protein-coupled receptor, class C, group 5, member D	20.66

B, Intermediate filament

GenBank accession no.	Gene name	Gene full name	Fold downregulation
BC003472	KRT23	Keratin 23	2.67
BC129847	KRT24	Keratin 24	2.66
BC018391	KRT25	Keratin 25	6.56
BC116672	KRT26	Keratin 26	7.78
AB288231	KRT28	Keratin 28	4.28
BC117553	KRT32	Keratin 32	6.04
BC12542	KRT34	Keratin 34	101.08
BC100542	KRT35	Keratin 35	6.86
BC119521	KRT40	Keratin 40	10.11
BC125346	KRT71	Keratin 71	2.90
BC067067	KRT73	Keratin 73	4.34
BC107395	KRT77	Keratin 77	9.12
BC119366	KRT80	Keratin 80	2.21
AF312018	KRT81	Keratin 81	30.65
BC10897	KRT82	Keratin 82	10.18
BC152922	KRT85	Keratin 85	19.46
BC029257	KRT33A	Keratin associated protein 33A	39.26
NM_013570	KRT33B	Keratin associated protein 33B	4.79
NM_001085526	KRTAP1-2	Keratin associated protein 1-3	13.42
XM_894811	KRTAP3-1	Keratin associated protein 3-1	29.03
BC156698	KRTAP4-2	Keratin associated protein 4-2	19.09
NM_026834	KRTAP4-6	Keratin associated protein 4-6	24.72
BC115508	KRTAP4-7	Keratin associated protein 4-7	33.02
NM_001085547	KRTAP4-8	Keratin associated protein 4-8	43.14
NM_001085548	KRTAP4-9	Keratin associated protein 4-9	24.62
BC016249	KRTAP4-16	Keratin associated protein 4-16	42.20
NM_015809	KRTAP5-4	Keratin associated protein 5-4	19.54
NM_027771	KRTAP7-1	Keratin associated protein 7-1	137.50
AK133727	KRTAP8-1	Keratin associated protein 8-1	18.92
BC116210	KRTAP9-1	Keratin associated protein 9-1	11.56
BC156686	KRTAP9-3	Keratin associated protein 9-3	35.46
NM_001085527	KRTAP9-5	Keratin associated protein 9-5	12.10
BC116219	KRTAP15	Keratin associated protein 15	60.31
BC116200	KRTAP19-4	Keratin associated protein 19-4	10.75
BC115545	KRTAP19-3	Keratin associated protein 19-3	8.54
BC132612	KRTAP6-5	Keratin associated protein 6-5	14.96
BC132658	KRTAP16-3	Keratin associated protein 16-3	39.91
BC128283	KRTAP26-1	Keratin associated protein 26-1	6.51

Table II. Continued.

C, Lipid metabolic process

GenBank accession no.	Gene name	Gene full name	Fold downregulation
AK003689	LYPLA2	Lysophospholipase II	2.00
BC027524	PLA2G2E	Phospholipase A2, group IIE	2.60
BC148434	PLCH2	Phospholipase C eta 2	2.13
BC047281	AGPAT4	1-acylglycerol-3-phosphate O-acyltransferase 4	3.81
BC031987	AGPAT5	1-acylglycerol-3-phosphate O-acyltransferase 5	3.17
AK019476	SMPD3	Sphingomyelin Phosphodiesterase 3 neutral	2.15
AK088962	SMPD2	Sphingomyelin phosphodiesterase 2 neutral	2.10
BC013751	ALOX12E	Arachidonate lipoxygenase	3.90
BC043059	LASS5/Cers5	Epidermal ceramide synthase 5	2.82
BC075627	DGKK	Diacylglycerol kinase κ	3.89
BC021597	APOM	Apolipoprotein M	2.58
BC006863	FAAH	Fatty acid amide hydrolase	2.22
BC071266	FADS3	Fatty acid desaturase 3	2.53

D, Gap junction

GenBank accession no.	Gene name	Gene full name	Fold downregulation
AY427554	GJA1	Gap junction protein α1	2.00
AY390399	GJA3	Gap junction protein α3	2.57
BC024387	GJB3	Gap junction protein β3	2.77

E, Tight junction

GenBank accession no.	Gene name	Gene full name	Fold downregulation
AK165750	PRKCZ	Protein kinase C ζ	2.37
DQ682659	MARVELD2	MARVEL domain containing 2	3.81
AK190015	TJAP1	Tight junction associated protein 1	2.08
BC049662	MPP7	Membrane palmitoylated protein 7	2.11

F, Desmosome

GenBank accession no.	Gene name	Gene full name	Fold downregulation
BC020144	DSG2	Desmoglein 2	4.48

in 'cornified envelope components', 'serine protease and protease inhibitors', 'lipid metabolic process', 'tight junction' and 'transcriptional factors' (Table III). The downregulated epidermal barrier-associated genes following treatment with ATRA in HaCaT cells included genes involved in 'intermediate filament', 'proteases and protease inhibitors' and 'tight junction' (Table IV). The upregulated epidermal barrier-associated genes following treatment with ATRA in HaCaT cells included genes involved in 'intermediate filament', 'proteases and protease inhibitors' and 'tight junction' (Table V).

The pathway analyses demonstrated that differentially expressed genes were significantly associated with AJs, TJs and focal adhesion in ATRA-treated epidermal tissues. The top ten pathways of up- and downregulated differentially expressed genes are presented in Fig. 4A and B, respectively. The top ten three GO-fold enrichment of differentially expressed genes revealed significant downregulation of epidermal barrier function-associated processes, including 'regulation of keratinocyte differentiation', 'keratin filament' and 'gap junction' channel activity (Fig. 4C-H). In ATRA-treated epidermal tissues, a series of dysregulated genes associated with the epidermal differentiation complex (EDC) were observed, which included small proline-rich region proteins (SPRRs), filaggrin (FLG), loricrin (LOR) and the S100 gene family. These proteins are essential for the formation of the cell envelope during terminal differentiation. A number of these genes were members of

Table III. Upregulation of epidermal barrier-associated genes following treatment with all-*trans* retinoic acid in the mouse skin (n=1 per group;-fold change >2; P<0.05).

A, Cornified envelope components

GenBank accession no.	Gene name	Gene full name	Fold upregulation
BC115788	LCE3B	Late cornified envelope 3B	3.17
BC119239	LCE3C	Late cornified envelope 3C	5.35
BC125542	SPRR2J	Small proline-rich protein 2J	2.38
BC130233	SPRR2G	Small proline-rich protein 2G	3.57
BC078629	S100A8	S100 calcium binding protein A8 (calgranulin A)	3.31
AK143826	S100A9	S100 calcium binding protein A9 (calgranulin B)	3.81

B, Serine protease and protease inhibitors

GenBank accession no.	Gene name	Gene full name	Fold upregulation
BC031119	KLK6	Kallikrein related-peptidase 6	3.22
BC002100	KLK10	Kallikrein related-peptidase 10	2.90
XM_893506	KLK12	Kallikrein related-peptidase 12	2.50
BC054091	SERPINE1	Serine (cysteine) proteinase inhibitor, clade E, member 1	2.15
BC010675	SERPINE2	Serine (cysteine) proteinase inhibitor, clade E, member 2	2.98

C, Lipid metabolic process

GenBank accession no.	Gene name	Gene full name	Fold upregulation
BC010829	ACNAT2	Acyl-coenzyme A amino acid N-acyltransferase 2	2.03
DQ469311	ACNAT1	Acyl-coenzyme A amino acid N-acyltransferase 1	2.94
AK171255	ACOT11	Acyl-CoA thioesterase 11	3.73
BC050828	UGCG	UDP-glucose ceramide glucosyltransferase	2.21
BC060600	PLA2G4E	Phospholipase A2, group IVE	2.39
BC003470	PLA1A	Phospholipase A1 member A	2.06
BC003943	DPAGT1	Dolichyl-phosphate (UDP-N-acetylglucosamine) glycerol	2.10

D, Tight junction

GenBank accession no.	Gene name	Gene full name	Fold upregulation
BC015252	CLDN2	Claudin-2	2.43

E, Transcriptional factors

GenBank accession no.	Gene name	Gene full name	Fold upregulation
BC070398	PPARδ	Peroxisome proliferator activator receptor δ	2.00

the SPRR family: *SPRR4* (-2.67-fold), *SPRR2J* (+2.38-fold) and *SPRR2G* (+3.57-fold). The remainder were part of the S100 gene family: *S100A8* (+3.31-fold) *S100A9* (+3.81-fold) and *FLG* (-2.13-fold) (Tables II and III). During keratinocyte differentiation, the late cornified envelope protein (LCE) was induced and had similar functions to the functions of the SPRR family (cross-linking proteins) in the CE. *LCE1M* (6.64-fold) was downregulated, while *LCE3C* (5.35-fold) and *LCE3B* (3.17-fold) were upregulated (Tables II and III). Nevertheless, no notable abnormalities were observed in the above genes in HaCaT cells. In ATRA-treated epidermal tissues and HaCaT cells, marked dysregulation of numerous keratins and keratin-associated proteins was observed, suggesting abnormal terminal differentiation of keratinocytes upon ATRA treatment. Serine proteases and serine protease inhibitors are involved in the differentiation of keratinocytes

Table IV. Downregulation of epidermal barrier-associated genes following treatment with all-*trans* retinoic acid in HaCaT cells (n=1 per group;-fold change >2; P<0.05).

A, Intermediate filament

GenBank accession no.	Gene name	Gene full name	Fold downregulation
NM_181619	KRTAP21-1	Keratin associated protein 21-1	2.38
NM_033448	KRT71	Keratin 71	2.00
BC024292	KRT5	Keratin 5	2.22

B, Proteases and protease inhibitors

GenBank accession no.	Gene name	Gene full name	Fold downregulation
BC069417	SERPINB7	Serpin family B member 7	3.15
NM_000185	SERPIND1	Serpin family D member 1	2.36
NM_007173	PRSS23	Serine protease 23	4.13
NM_022046	KLK14	Kallikrein related peptidase 10	2.29

C, Tight junction

GenBank accession no.	Gene name	Gene full name	Fold downregulation
AK128686	PDZD2	PDZ domain containing 2	2.15

and desquamation (24). In ATRA-treated epidermal tissues and HaCaT cells, the differential expression of serine proteases and serine protease inhibitors was observed. Among them, it was observed that KLK6 and KLK10 were consistently expressed in the mouse chip and HaCaT cells, and all of them were upregulated.

Genes encoding enzymes associated with lipid metabolism were demonstrated to be induced by ATRA in the mouse epidermis. Compared with the cells, the mice exhibited significant downregulation of a subset of enzymes associated with ceramide, free fatty acids and phospholipid synthesis: i) Sphingomyelin phosphodiesterase 3 (*SMPD3*; -2.15-fold) and sphingomyelin phosphodiesterase 2 (*SMPD2*, -2.10-folds), which catalyze the conversion of sphingolipids to ceramides; ii) epidermal ceramide synthase 5 (*LASS5*/*Cers5*; -2.82-fold), which catalyzes the synthesis of ceramides; iii) lysophospholipase II (*LYPLA*; -2.00-fold), phospholipase A2 group IIE2 (*PLA2G2E*; -2.60-fold), and phospholipase C eta 2 (*PLCH2*; -2.13-fold), which catalyze free fatty acid formation from phospholipids; and iv) 1-acylglycerol-3-phosphate O-acyltransferase 4 (*AGPAT4*; -3.81-fold) and 1-acylglycerol-3-phosphate O-acyltransferase 5 (*AGPAT5*; -3.17-fold), which catalyze the acylation of lysophosphatidic acid into phosphatidic acid. The latter is the primary precursor of all types of glycerolipids. Furthermore, arachidonate lipoxygenase (*ALOX12E*; a member of the epidermis-type LOX family that catalyzes the conversion of polyunsaturated fatty acids into oxygenated products) was downregulated by ATRA. Conversely, the present results also demonstrated upregulation of different isoforms of the aforementioned enzymes (Table III).

The dysregulation of numerous cell-cell junction-associated genes was observed in ATRA-treated mouse skin. Among these genes were components of TJs (*TJAP1*, *MPP7*, *MARVELD2* and *CLDN2*), gap junctions (*GJA, GJA* and *GJB4*) and desmosomes (*DSG2*). Compared with the mouse skin specimens, only the TJ protein molecules Claudin-4 and occludin were upregulated in the cells.

ATRA treatment alters the expression and localization of TJs in HaCaT cells. In ATRA-treated cells, *CLDN1* was downregulated 0.66-fold, while *CLDN4*, *TJP3* and *GJB4* were upregulated 1.82-, 3.63- and 1.92-fold (Fig. 5A). In mice treated with ATRA, *CLDN1* (0.8-fold) and *FLG* (0.61-fold) were downregulated, while *CLDN4* (1.47-fold) and *CLDN2* (2.49-fold) were upregulated (Fig. 5B). Western blot analysis of CLDN4 and CLDN1 revealed similar results to those of the RT-qPCR (Fig. 5C).

Immunofluorescence revealed that the intensity of Claudin-1 was not only reduced at the cell-cell contact areas, but also appeared to be discontinuous along the cell membranes of HaCaT cells treated with ATRA (Fig. 6). However, Claudin-4 staining was slightly increased and displayed a string-like localization pattern (Fig. 6).

ATRA alters the expression and localization of TJs in mouse epidermis. A marked reduction in the staining intensity and localization of Claudin-1 in the upper epidermal layer of skin treated with ATRA was discovered compared with control skin (n=3; Fig. 7). By contrast, Claudin-4 staining was stronger in the ATRA-treated skin compared with control skin (Fig. 7).

Table V. Upregulation of epidermal barrier-associated genes following treatment with all-*trans* retinoic acid in HaCaT cells (n=1 per group;-fold change >2; P<0.05).

A, Intermediate filament

GenBank accession no.	Gene name	Gene full name	Fold upregulation
NM_002275	KRT15	Keratin 15	2.07
BC072018	KRT17	Keratin 17	2.68
AB096945	KRTAP19-4	Keratin associated protein 19-4	2.07
BC101555	KRTAP7-1	Keratin associated protein 7-1 (gene/pseudogene)	2.05
NM_032524	KRTAP4-4	Keratin associated protein 4-4	2.16

B, Proteases and protease inhibitors

GenBank accession no.	Gene name	Gene full name	Fold upregulation
NM_001085	SERPINA3	Serpin family A member 3	12.30
NM_000624	SERPINA5	Serpin family A member 5	2.03
BC034528	SERPINB8	Serpin family B member 8	2.11
NM_000934	SERPINF2	Serpin family F member 2	2.06
NM_002575	SERPINB2	Serpin family B member 2	2.17
BC009726	PRSS22	Serine protease 22	4.26
AF335478	KLK3	Kallikrein related peptidase 3	2.27
NM_001012964	KLK6	Kallikrein related peptidase 6	2.95
NM_002776	KLK10	Kallikrein related peptidase 10	2.44
NM_006853	KLK11	Kallikrein related peptidase 11	2.43
NM_015596	KLK13	Kallikrein related peptidase 13	2.80
NM_017509	KLK15	Kallikrein related peptidase 15	2.02

C, Tight junction

GenBank accession no.	Gene name	Gene full name	Fold upregulation
BC029886	OCLN	Occludin	2.63
NM_001305	CLDN4	Claudin-4	2.02

Discussion

In the present study, the ATRA-associated dermatitis animal model presented erythema, scaling and dryness of the treated skin, similar to the irritation observed in ATRA-treated human skin (25,26), indicating that this animal model is a useful tool to evaluate the effectiveness and side effects of ATRA. Furthermore, treatment with ATRA altered the normal morphology and ultrastructure of the mouse epidermis. Microarray analysis was used, primarily to identify candidates that were later confirmed via RT-qPCR and/or immunohistochemistry.

In the mouse model of ATRA-stimulated dermatitis, the epidermis of the mice exhibited obvious scales, while histopathology revealed parakeratosis of the epidermis, suggesting that the epidermal differentiation was abnormal, and that the abnormal differentiation of keratinocytes led to an epidermal keratinization envelope. In the mouse gene expression profiles, it was observed that the majority of alterations occurred among EDC genes, including *FLG*, *SPRR4*, *SPRR2J*, *SPRR2G*, *LCE3C*, *LCE3B*, *LCE1M*, *S100A8* and *S100A9*. The proteins encoded by those genes, together with LOR, involucrin, trichohyalin and hornerin, are associated with CE generation via crosslinking of insoluble membranous proteins (27). Keratinized proteins act as markers of differentiation in the epidermis. In the mice and cells, the abnormal expression of keratins, including *KRT15*, *KRT17* and *KRT14*, and keratin-associated proteins, including *KRT33A*, *KRT33A* and *KRTAP1-3*, was widely observed, further confirming the abnormal terminal differentiation in the epidermis following ATRA treatment.

Proteases, together with their inhibitors and targets, serve an essential role in desquamation (24). In the ATRA-treated mouse epidermis and HaCaT cells, the upregulation of tissue kallikreins (*KLK6*, *KLK10*, *KLK12* and *KLK14*) and protease inhibitors (*SERPINE 1* and *SERPINE 2*) was demonstrated. It is noteworthy that KLK6 and KLK10 were upregulated in mice and cells following ATRA treatment, which may be

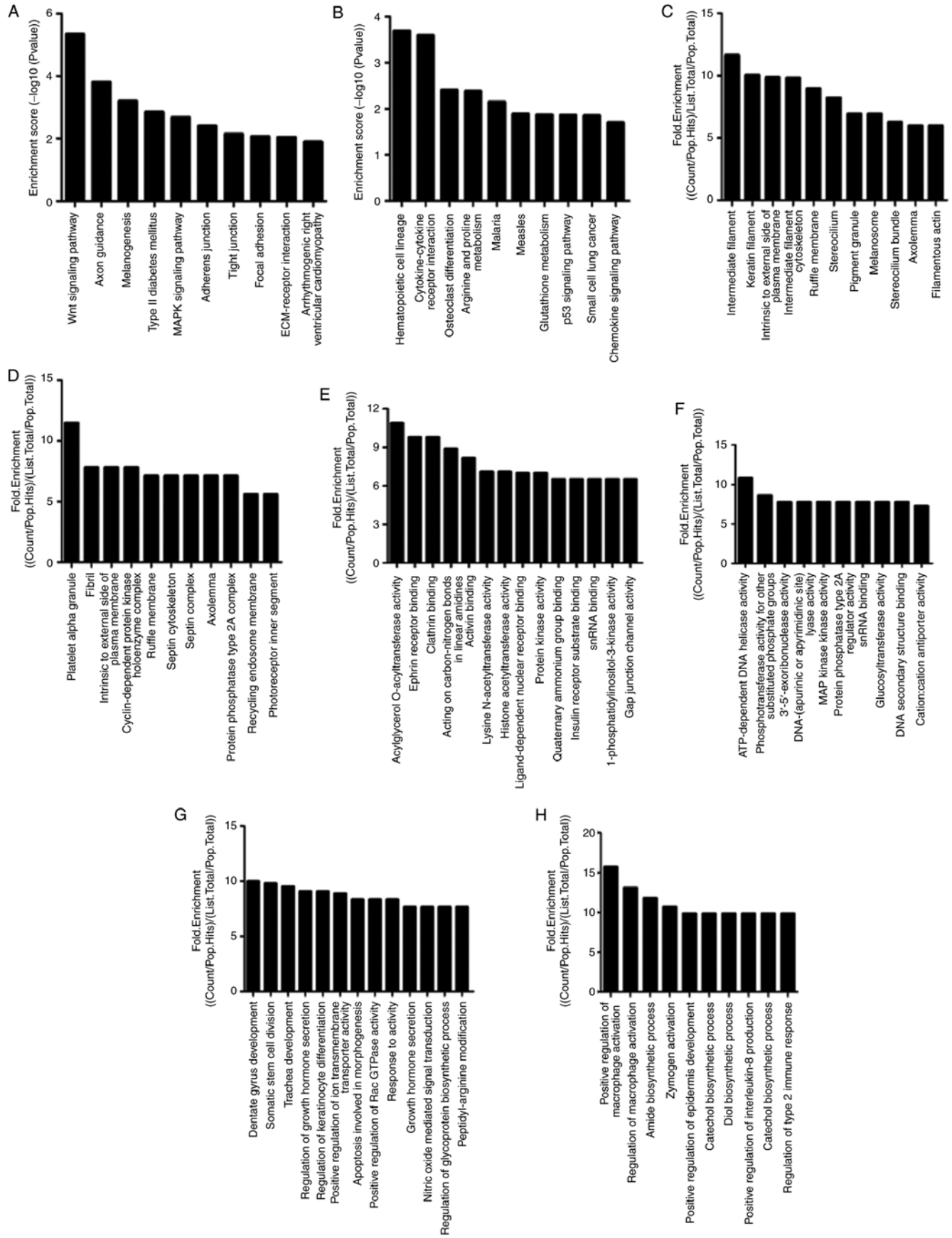

Figure 4. Top ten pathways of up- and downregulated genes. The bar plots indicate the top ten (A) down- and (B) upregulated enrichment score [$-\log_{10}{}^{(\text{P-value})}$] values of the significantly enriched pathways (n=1 per group). The top ten (C) down- and (D) upregulated-fold enrichment [(Count/Pop.Hits)/(List.Total/Pop.Total)] values of the significant biological processes are presented. The bar plots indicated the top ten (E) down- and (F) upregulated-fold enrichment [(Count/Pop.Hits)/(List.Total/Pop.Total)] values of the significant cellular components. The top ten (G) down- and (H) upregulated-fold enrichment [(Count/Pop.Hits)/(List.Total/Pop.Total)] values of the significant molecular functions are presented. Count, the number of differentially expressed genes associated with the listed GOID; Pop.Hits, the number of background population genes associated with the listed GOID; List.Total, the total number of differentially expressed genes; and Pop.Total, the total number of background population genes. GO, Gene Ontology.

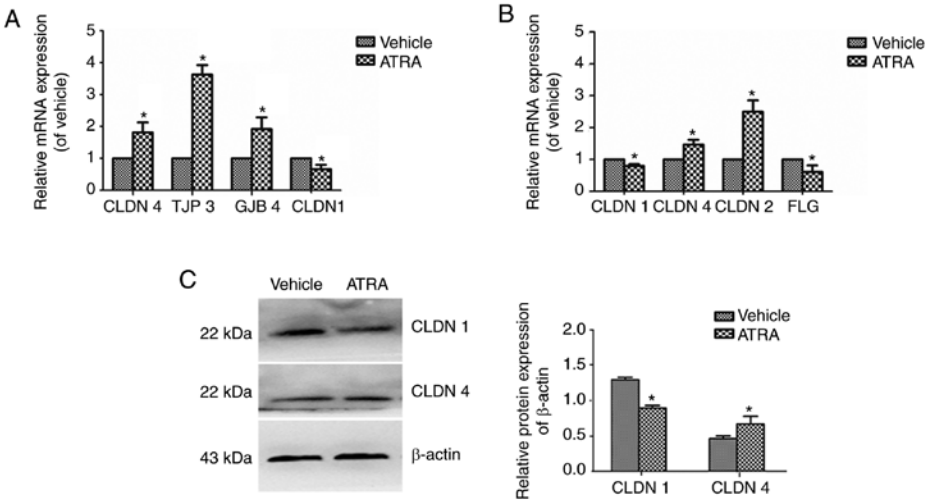

Figure 5. mRNA and protein expression levels of CLDN1 and CLDN4 in immortalized keratinocyte HaCaT cells treated with ATRA. HaCaT cells were incubated with or without 1 μM ATRA for 36 h. (A) In the cells, CLDN-4, TJP3 and JGB4 were upregulated, while CLDN1 was downregulated. (B) In mice, CLDN1 and FLG were downregulated, while CLDN4 and CLDN2 were upregulated. (C) CLDN1 and CLDN4 protein expression levels were determined by western blotting. β-actin was used as a loading control. Data are presented as the mean ± standard deviation from three independent experiments performed in triplicate (n=3). *P<0.05 vs. respective vehicle group. CLDN, Claudin; ATRA, all-*trans* retinoic acid; TJP3, tight junction protein 3; GJB4, gap junction protein β4; FLG, filaggrin.

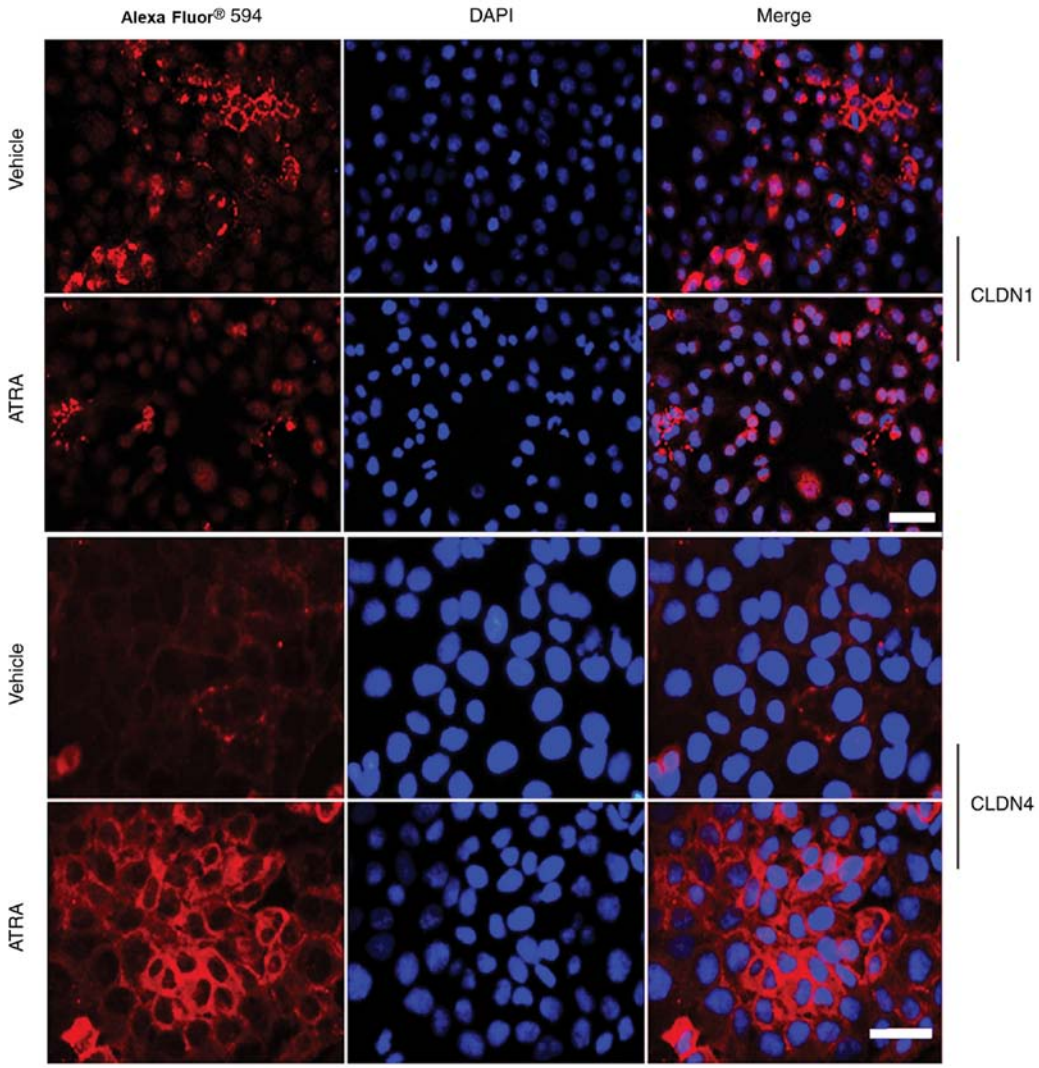

Figure 6. Localization and expression of CLDN1 and CLDN4 in cultured HaCaT cells treated with ATRA. The localization of CLDN4 and CLDN1 (both red) was observed at the intercellular border in a string-like pattern in HaCaT cells treated with the vehicle. In ATRA-treated cells, CLDN4 immunofluorescence at the cell-cell contact sites appeared to be more intense compared with that in the vehicle group, while CLDN1 exhibited increased punctate localization in ATRA-treated cells. DAPI was used as a counterstain (blue). Scale bar, 20 μm. CLDN, Claudin; ATRA, all-*trans* retinoic acid.

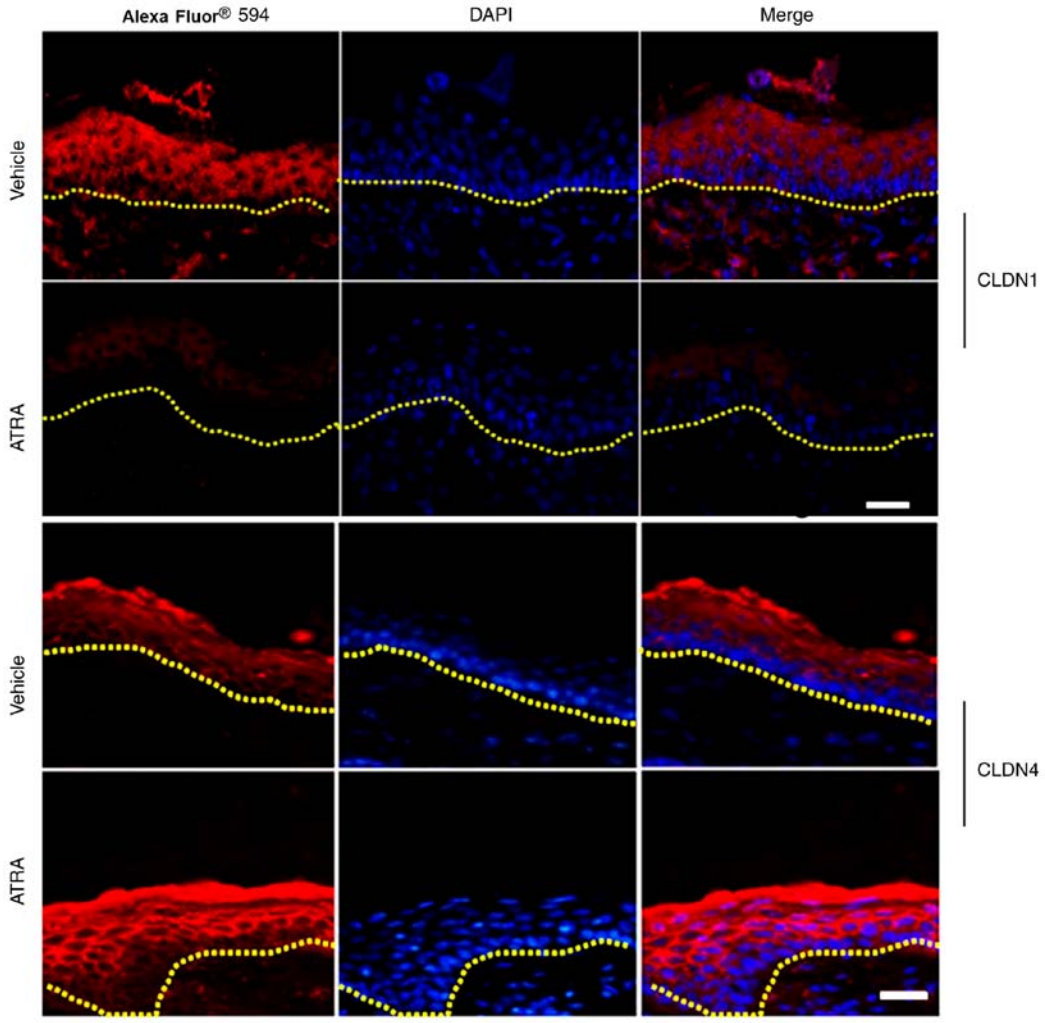

Figure 7. Effect of ATRA on the localization and expression of CLDN1 and CLDN4 in mouse epidermal tissues. Following ATRA treatment, CLDN1 (red) was expressed at the cell-cell borders in the granular and spinous layers, but disappeared from the basal layers. CLDN4 (red) was expressed at the cell-cell borders in the granular layer and was enhanced in the upper spinous layer and granular layer following treatment with ATRA. DAPI was used as a counterstain (blue). Dotted lines indicate the basal layer. Scale bar, 20 μm. n=3 per group. A representative image was selected from each group. CLDN, Claudin; ATRA, all-*trans* retinoic acid.

closely associated with the appearance of scales on the mouse skin. Furthermore, alterations in the balance between proteases and protease inhibitors in the skin lead to inflammatory reactions, which causes itching, scaling, redness and other typical clinical symptoms (28).

Morphologically, the appearance of profilaggrin is consistent with the formation of keratohyalin granules. The newly-synthesized profilaggrin accumulates in keratohyalin granules with high phosphoric acid and histidine following phosphorylation. The present study demonstrated that the number of keratohyalin granules decreased significantly following ATRA treatment. Therefore, it was speculated that decreases in the number of keratohyalin granules may affect the phosphorylation and accumulation of newly-synthesized profilaggrin, affecting the production of FLG. In addition, a number of factors that are important in controlling FLG expression have been described, such as transcription factors of the AP1 family (Jun and/or Fos), POU-domain proteins, transcription factor p63, and the peroxisome-proliferator-activated-receptor (PPAR) family (29). Aberrant profilaggrin processing has also been observed in 12R-lipoxygenase (12R-LOX)-deficient mice (30). In the present study, the gene chip results revealed that PPAR was upregulated and *ALOX12E* was downregulated following ATRA treatment. As expected, the gene chip analysis and RT-qPCR revealed that the expression of *FLG* was downregulated following ATRA treatment in the mouse skin, as supported by Sybert *et al* (31), who reported that patients with ichthyosis vulgaris displayed a reduction or absence of profilaggrin and FLG along with a morphological reduction in the amount of keratohyalin. Filaggrin is also involved in the production of primary natural moisturizing factors in the stratum corneum (29). Whether these alterations in expression may affect the expression of FLG and the specific regulatory mechanism requires further investigation.

Following ATRA treatment, alterations in the ultrastructure of the epidermis were observed under an electron microscope. The images revealed that there were numerous circular vacuolated structures in the stratum corneum, which were similar to the ultrastructure of lipid droplets. Ponec *et al* (32) studied the lipid and ultrastructure of reconstructed skin models by electron microscopy. Their results indicated that lipid droplets in keratinocytes appeared in all three skin models, but the

extent of the lipid droplets varied. The structure of the lipid droplets in their images was consistent with the structure of lipid droplets observed under electron microscopy in the present study. It was also thought that the different levels of lipid droplets in keratinocytes were associated with the hyperproliferative state of reconstructed skin. On the other hand, the epidermal layers of the mice in the present study were increased following ATRA treatment, indicating that there was a degree of proliferation. Therefore, it was speculated that these structures may be lipid droplets. Nevertheless, this is a limitation of the present study.

The ATRA-treated mouse skin displayed a large number of lipid droplets in certain corneocytes [similar in appearance to the droplets observed by Ponec *et al* (32)], suggesting that lipid metabolism was abnormal. Gene expression analysis of skin samples from ATRA-treated and control skin demonstrated significant induction of functional proteins associated ceramide, non-esterified fatty acids and phospholipid synthesis. The present study revealed downregulation of *SMPD3*, *SMPD2* and *LASS5*/*Cers5*, which catalyze the synthesis of ceramides, suggesting decreased ceramide synthesis in ATRA-treated mice. Conversely, it was observed that ATRA also increased the expression of UDP-glucose ceramide glucosyltransferase (UGCG). Moreover, Amen *et al* (33) reported that mice with deficiencies in UGCG display an ichthyosis-like skin phenotype and impairment in the differentiation of keratinocytes, which is associated with delayed wound healing.

Mao-Qiang *et al* (34) demonstrated that inhibiting *PLA2* resulted in a defective extracellular lipid membrane and impaired homeostasis in the permeability barrier (34). In the present study, ATRA not only downregulated *PLA2G2E* and other phospholipases including *PLCH2,* but also upregulated *PLA2G4E*, *LYPLA* and *DEG*. Lu *et al* (35) demonstrated that the transcription levels of AGPAT-1, -2 and -3 were rapidly increased by ATRA. The present gene expression analysis of ATRA-treated skin revealed a marked reduction in the levels of *AGPAT4* and *AGPAT5*.

Previously, lipoxygenases (LOXs) were reported to exert essential roles in regulating epithelial proliferation and/or differentiation, maintaining the permeability barrier, skin inflammation and wound healing (36). In the present study, no marked alterations in the protein levels of *eLOX-3* and *12R-LOX* in ATRA-treated skin were detected, but ATRA-treatment significantly downregulated *ALOX12E*, which may have a role in regulating keratinocyte differentiation (37).

TEM analysis of the mouse skin revealed an increase in the intercellular space, suggesting that the keratinocytes of the mice may have had abnormalities in the TJs. TJs function as a paracellular barrier beneath the stratum corneum (38). In the present study, Claudin-1 was decreased, but Claudin-4 was increased following ATRA-treatment in HaCaT cells and the mouse epidermis. Claudin-1-knockout mice exhibit increased epidermal permeability, severe water loss and skin wrinkling, and succumb within 24 h after birth (17). Downregulation of Claudin-1 results in decreased transepithelial electrical resistance (39). In addition, patients with atopic dermatitis exhibit low levels of Claudin-1 expression (40). Nevertheless, a previous *in vitro* study of cultured keratinocytes uncovered barrier defects resulting from knocking down Claudin-4 (41). The present study revealed that the expression of Claudin-4 was increased following ATRA treatment in HaCaT cells and the mouse epidermis, as previously observed in the oral mucosa (14). Nevertheless, significant upregulation of Claudin-4 was observed in the non-lesional skin of patients with atopic dermatitis, which may indicate a compensatory response to disrupted barrier function caused by Claudin-1 downregulation that leads to the upregulation of other Claudins (18,42). Therefore, downregulated Claudin-1 and the alteration of its localization in HaCaT cells and the mouse epidermis was likely responsible, at least in part, for the observed disruption of TJ barrier function following ATRA treatment.

It was observed that Claudin-2 mRNA was upregulated 2.5-fold. Telgenhoff *et al* (43) studied the regulation of Claudin-2 mRNA and protein expression by ATRA in human keratinocytes, and discovered that ATRA increases the expression of Claudin-2 in keratinocytes in a dose-dependent manner. In addition, Claudin-2 is highly expressed in the TJs of mouse renal proximal tubules, which possess a leaky epithelium whose unique permeability properties underlie their high rate of NaCl reabsorption (43,44). On the other hand, the Cldn2-KO mice display a normal appearance, activity, growth and behavior, with no abnormalities in the epidermal barrier (44); therefore, it was not included in the present study as a candidate gene due to funding limitations, but it may be considered in future studies.

Notably, certain differences were observed between the *in vivo* and the *in vitro* experiments. The possible causes include the following: i) HaCaT cells are human-derived immortalized keratin-forming cells, while the skin tissues were derived from mice, thus the two are different in species; ii) cells growing *in vitro* and *in vivo* are not completely analogous; and iii) the doses of ATRA *in vivo* and *in vitro* were different. In addition, the present study is limited since it focused primarily on Claudin-1 and -4, and additional studies are required to assess the exact contribution to ATRA-induced dermatitis of all the identified differentially expressed genes. The microarray experiment would ideally have been performed in multiple samples, but research funding was very limited; thus, there was only one sample per group, which is a limitation. Nevertheless, the microarray experiment only provides an idea of the potential genes that may be examined in future studies. Subsequent experiments *in vivo* and *in vitro* will be performed to confirm the results.

In conclusion, the results suggest that ATRA disrupts the normal morphology and ultrastructure of the mouse epidermis and exerts an essential role in the function of the epidermal barrier. Gene expression analyses revealed numerous dysregulated genes associated with the synthesis/generation of transcription factors, protease inhibitors, proteases, junctional proteins, lipids, corneocytes and cornified envelopes. ATRA not only alters the expression of Claudin-1 and -4, but also alters their localization in HaCaT cells and the murine epidermis. ATRA exerts a dual effect on epidermal barrier genes: It downregulates the expression of Claudin-1 and upregulates the expression of Claudin-4. Claudin-4 upregulation may be a compensatory response for the disrupted barrier function caused by Claudin-1 downregulation.

Acknowledgements

Not applicable.

Funding

The present study was supported by the National Natural Science Foundation of China (grant no. 81171490) and the Fundamental Research Funds for the Central Universities (grant no. PY3A0241001016).

Availability of data and materials

The datasets generated and/or analyzed during the current study are available in the GEO repository (GSE124183): https://www.ncbi.nlm.nih.gov/geo/query/acc.cgi?acc=GSE124183.

Authors' contributions

SG and JL designed the experiments. JL conducted the experiments, performed the statistical analysis and drafted the manuscript. QL performed the statistical analysis. All authors read and approved the final manuscript.

Ethics approval and consent to participate

All experimental procedures were performed in accordance with the 'Principles of Laboratory Animal Care' (National Institutes of Health) and the guidelines of the laboratory animal care committee of Xi'an Jiaotong University (no. XJTULAC2017-733).

Patient consent for publication

Not applicable.

Competing interests

All authors declare that they have no competing interests.

References

1. Ahuja HS, Szanto A, Nagy L and Davies PJ: The retinoid X receptor and its ligands: Versatile regulators of metabolic function, cell differentiation and cell death. J Biol Regul Homeost Agents 17: 29-45, 2003.
2. Wilson L, Gale E and Maden M: The role of retinoic acid in the morphogenesis of the neural tube. J Anat 203: 357-368, 2003.
3. Thielitz A and Gollnick H: Topical retinoids in acne vulgaris: Update on efficacy and safety. Am J Clin Dermatol 9: 369-381, 2008.
4. Torma H, Bergström A, Ghiasifarahani G and Berne B: The effect of two endogenous retinoids on the mRNA expression profile in human primary keratinocytes, focusing on genes causing autosomal recessive congenital ichthyosis. Arch Dermatol Res 306: 739-747, 2014.
5. Zhang ML, Tao Y, Zhou WQ, Ma PC, Cao YP, He CD, Wei J and Li LJ: All-*trans* retinoic acid induces cell-cycle arrest in human cutaneous squamous carcinoma cells by inhibiting the mitogen-activated protein kinase-activated protein 1 pathway. Clin Exp Dermatol 39: 354-360, 2014.
6. Ale SI, Laugier JP and Maibach HI: Differential irritant skin responses to tandem application of topical retinoic acid and sodium lauryl sulphate: Ii. Effect of time between first and second exposure. Br J Dermatol 137: 226-233, 1997.
7. Kirschner N, Houdek P, Fromm M, Moll I and Brandner JM: Tight junctions form a barrier in human epidermis. Eur J Cell Biol 89: 839-842, 2010.
8. Brandner JM: Importance of tight junctions in relation to skin barrier function. Curr Probl Dermatol 49: 27-37, 2016.
9. Furuse M, Sasaki H, Fujimoto K and Tsukita S: A single gene product, claudin-1 or -2, reconstitutes tight junction strands and recruits occludin in fibroblasts. J Cell Biol 143: 391-401, 1998.
10. Furuse M and Tsukita S: Claudins in occluding junctions of humans and flies. Trends Cell Biol 16: 181-188, 2006.
11. Turksen K and Troy TC: Permeability barrier dysfunction in transgenic mice overexpressing claudin 6. Development 129: 1775-1784, 2002.
12. Troy TC, Rahbar R, Arabzadeh A, Cheung RM and Turksen K: Delayed epidermal permeability barrier formation and hair follicle aberrations in inv-cldn6 mice. Mech Dev 122: 805-819, 2005.
13. Sugawara T, Iwamoto N, Akashi M, Kojima T, Hisatsune J, Sugai M and Furuse M: Tight junction dysfunction in the stratum granulosum leads to aberrant stratum corneum barrier function in claudin-1-deficient mice. J Dermatol Sci 70: 12-18, 2013.
14. Hatakeyama S, Ishida K and Takeda Y: Changes in cell characteristics due to retinoic acid; specifically, a decrease in the expression of claudin-1 and increase in claudin-4 within tight junctions in stratified oral keratinocytes. J Periodontal Res 45: 207-215, 2010.
15. Anderson JM and Van Itallie CM: Physiology and function of the tight junction. Cold Spring Harb Perspect Biol 1: a002584, 2009.
16. Furuse M: Knockout animals and natural mutations as experimental and diagnostic tool for studying tight junction functions in vivo. Biochim Biophys Acta 1788: 813-819, 2009.
17. Furuse M, Hata M, Furuse K, Yoshida Y, Haratake A, Sugitani Y, Noda T, Kubo A and Tsukita S: Claudin-based tight junctions are crucial for the mammalian epidermal barrier: A lesson from claudin-1-deficient mice. J Cell Biol 156: 1099-1111, 2002.
18. Gruber R, Börnchen C, Rose K, Daubmann A, Volksdorf T, Wladykowski E, Vidal-Y-Sy S, Peters EM, Danso M, Bouwstra JA, *et al*: Diverse regulation of claudin-1 and claudin-4 in atopic dermatitis. Am J Pathol 185: 2777-2789, 2015.
19. Tokumasu R, Yamaga K, Yamazaki Y, Murota H, Suzuki K, Tamura A, Bando K, Furuta Y, Katayama I and Tsukita S: Dose-dependent role of claudin-1 in vivo in orchestrating features of atopic dermatitis. Proc Natl Acad Sci USA 113: E4061-E4068, 2016.
20. Tokumasu R, Tamura A and Tsukita S: Time- and dose-dependent claudin contribution to biological functions: Lessons from claudin-1 in skin. Tissue Barriers 5: e1336194, 2017.
21. Bożek A and Reich A: The reliability of three psoriasis assessment tools: Psoriasis area and severity index, body surface area and physician global assessment. Adv Clin Exp Med 26: 851-856, 2017.
22. Fisher G, Esmann J, Griffiths CE, Talwar HS, Duell EA, Hammerberg C, Elder JT, Finkel LJ, Karabin GD, Nickoloff BJ, *et al*: Cellular, immunologic and biochemical characterization of topical retinoic acid-treated human skin. J Invest Dermatol 96: 699-707, 1991.
23. Livak KJ and Schmittgen TD: Analysis of relative gene expression data using real-time quantitative PCR and the 2(-Delta Delta C(T)) method. Methods 25: 402-408, 2001.
24. Ovaere P, Lippens S, Vandenabeele P and Declercq W: The emerging roles of serine protease cascades in the epidermis. Trends Biochem Sci 34: 453-463, 2009.
25. Phillips TJ: An update on the safety and efficacy of topical retinoids. Cutis 75: 14-22, 24; discussion 22-23, 2005.
26. Weiss JS, Shavin JS, Nighland M and Grossman R: Tretinoin microsphere gel 0.1% for photodamaged facial skin: A placebo-controlled trial. Cutis 78: 426-432, 2006.
27. Marshall D, Hardman MJ, Nield KM and Byrne C: Differentially expressed late constituents of the epidermal cornified envelope. Proc Natl Acad Sci USA 98: 13031-13036, 2001.
28. Meyer-Hoffert U: Reddish, scaly, and itchy: How proteases and their inhibitors contribute to inflammatory skin diseases. Arch Immunol Ther Exp (Warsz) 57: 345-354, 2009.
29. Sandilands A, Sutherland C, Irvine AD and McLean WH: Filaggrin in the frontline: Role in skin barrier function and disease. J Cell Sci 122: 1285-1294, 2009.
30. Epp N, Fürstenberger G, Muller K, de Juanes S, Leitges M, Hausser I, Thieme F, Liebisch G, Schmitz G and Krieg P: 12r-lipoxygenase deficiency disrupts epidermal barrier function. J Cell Biol 177: 173-182, 2007.

31. Sybert VP, Dale BA and Holbrook KA: Ichthyosis vulgaris: Identification of a defect in synthesis of filaggrin correlated with an absence of keratohyaline granules. J Invest Dermatol 84: 191-194, 1985.
32. Ponec M, Boelsma E, Weerheim A, Mulder A, Bouwstra J and Mommaas M: Lipid and ultrastructural characterization of reconstructed skin models. Int J Pharm 203: 211-225, 2000.
33. Amen N, Mathow D, Rabionet M, Sandhoff R, Langbein L, Gretz N, Jäckel C, Grone HJ and Jennemann R: Differentiation of epidermal keratinocytes is dependent on glucosylceramide: Ceramide processing. Hum Mol Genet 22: 4164-4179, 2013.
34. Mao-Qiang M, Jain M, Feingold KR and Elias PM: Secretory phospholipase A2 activity is required for permeability barrier homeostasis. J Invest Dermatol 106: 57-63, 1996.
35. Lu B, Jiang YJ, Man MQ, Brown B, Elias PM and Feingold KR: Expression and regulation of 1-acyl-sn-glycerol- 3-phosphate acyltransferases in the epidermis. J Lipid Res 46: 2448-2457, 2005.
36. Krieg P and Fürstenberger G: The role of lipoxygenases in epidermis. Biochim Biophys Acta 1841: 390-400, 2014.
37. Feingold KR: Thematic review series: Skin lipids. The role of epidermal lipids in cutaneous permeability barrier homeostasis. J Lipid Res 48: 2531-2546, 2007.
38. Yuki T, Haratake A, Koishikawa H, Morita K, Miyachi Y and Inoue S: Tight junction proteins in keratinocytes: Localization and contribution to barrier function. Exp Dermatol 16: 324-330, 2007.
39. Yamamoto T, Saeki Y, Kurasawa M, Kuroda S, Arase S and Sasaki H: Effect of RNA interference of tight junction-related molecules on intercellular barrier function in cultured human keratinocytes. Arch Dermatol Res 300: 517-524, 2008.
40. De Benedetto A, Rafaels NM, McGirt LY, Ivanov AI, Georas SN, Cheadle C, Berger AE, Zhang K, Vidyasagar S, Yoshida T, *et al*: Tight junction defects in patients with atopic dermatitis. J Allergy Clin Immunol 127: 773-786 e1-7, 2011.
41. Kirschner N, Rosenthal R, Furuse M, Moll I, Fromm M and Brandner JM: Contribution of tight junction proteins to ion, macromolecule, and water barrier in keratinocytes. J Invest Dermatol 133: 1161-1169, 2013.
42. Kubo T, Sugimoto K, Kojima T, Sawada N, Sato N and Ichimiya S: Tight junction protein claudin-4 is modulated via Δnp63 in human keratinocytes. Biochem Biophys Res Commun 455: 205-211, 2014.
43. Telgenhoff D, Ramsay S, Hilz S, Slusarewicz P and Shroot B: Claudin 2 mRNA and protein are present in human keratinocytes and may be regulated by all-trans-retinoic acid. Skin Pharmacol Physiol 21: 211-217, 2008.
44. Muto S, Hata M, Taniguchi J, Tsuruoka S, Moriwaki K, Saitou M, Furuse K, Sasaki H, Fujimura A, Imai M, *et al*: Claudin-2-deficient mice are defective in the leaky and cation-selective paracellular permeability properties of renal proximal tubules. Proc Natl Acad Sci USA 107: 8011-8016, 2010.